Electronic Supplementary Material (ESI) for Nanoscale Advances.

Supporting Information

Ultra-thin membrane filter without cake formation of a uniformly arrayed nanopore structure for the nanoscale separation of extracellular vesicles

Daesan Kim[1], Jaehyuk Lee[2], Boyoung Kim[2], Yujin Shin[2], Jinhong Park[3,4], Uijoo Kim[1, 5], Minbaek Lee[3,4] Sang Bum Kim[5] and Sunghoon Kim[1, 5]*

[1]Medicinal Bioconvergence Research Center, Institute for Artificial Intelligence and Biomedical Research, Yonsei University, Incheon 21983, Korea

[2]R&D Center, Metapore Co., Ltd, Advanced Institutes of Convergence Technology 8F, Suwon 16229, Korea

[3]Department of Physics, Inha University, Incheon 22212, Korea

[4]The Institute for Basic Science, Inha University, Incheon 22212, Korea

[5]College of Pharmacy & College of Medicine, Interdisciplinary Biomedical Center, Gangnam Severance Hospital, Yonsei University, Incheon 21983, Korea

[6]College of Pharmacy, Sahmyook University, Seoul 01795, Korea

SEM images of a commercial filter membrane

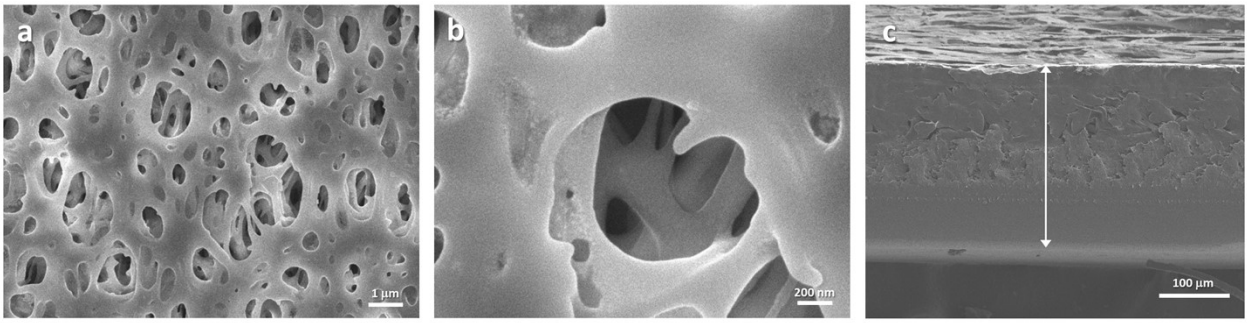

Figure S1. SEM image of a porous membrane. (a, b) Porous morphology of membrane surface. (c) Section profile of the porous membrane. The thickness of the membrane is about 260 μm.

Schematic diagram of fabrication of the NUTS

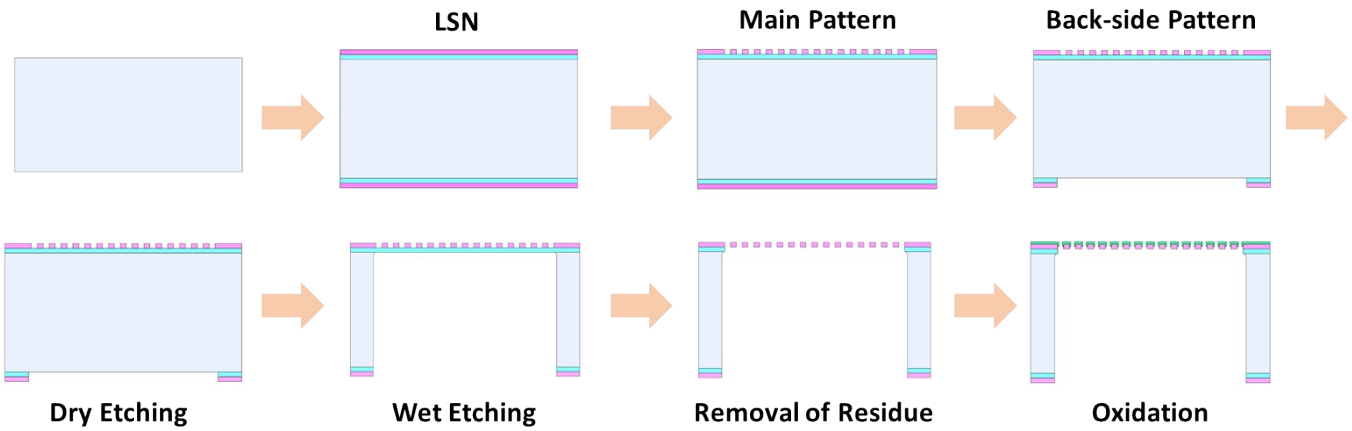

Figure S2. Schematic diagram of the fabrication of the NUTS.

Relationships of pressure with various factors

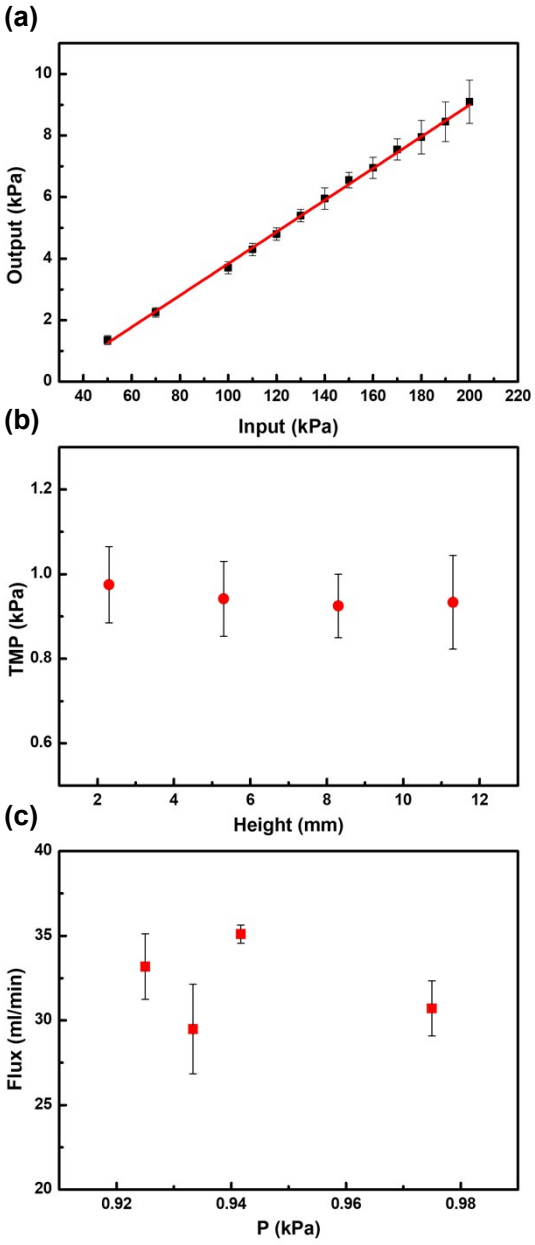

Figure S3. Relation of pressure on the membrane and filtrate flux in various conditions. (a) Pressure endurance test of the NUTS via N2 gas. The pressure range is from 50 to 200 kPa for the inlet line, with a linear response to the filtrate line at about 1–9 kPa. (b) Change in TMP with inlet height. TMP is approximately the same value under all conditions. (c) Change in flux with TMP. The flux is does not appear to change significantly with TMP.

Optical image of a NUTS surface

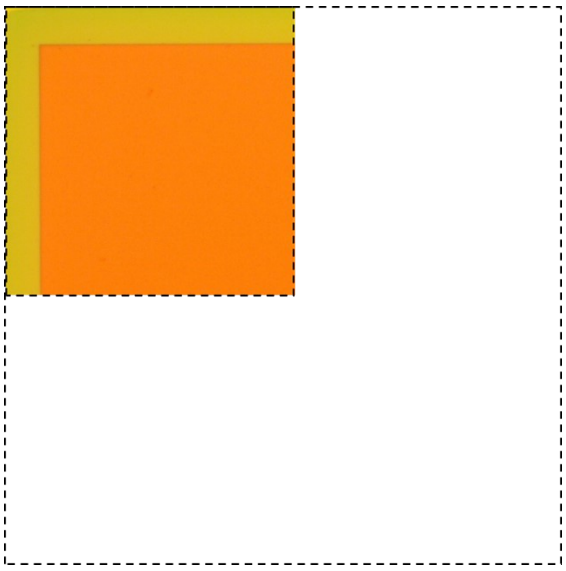

Figure S4. Optical image of a quarter of membrane. The total dimensions of a single membrane are 1 x 1 mm, and all membranes have the same size.

Distribution of pore diameter in single membrane

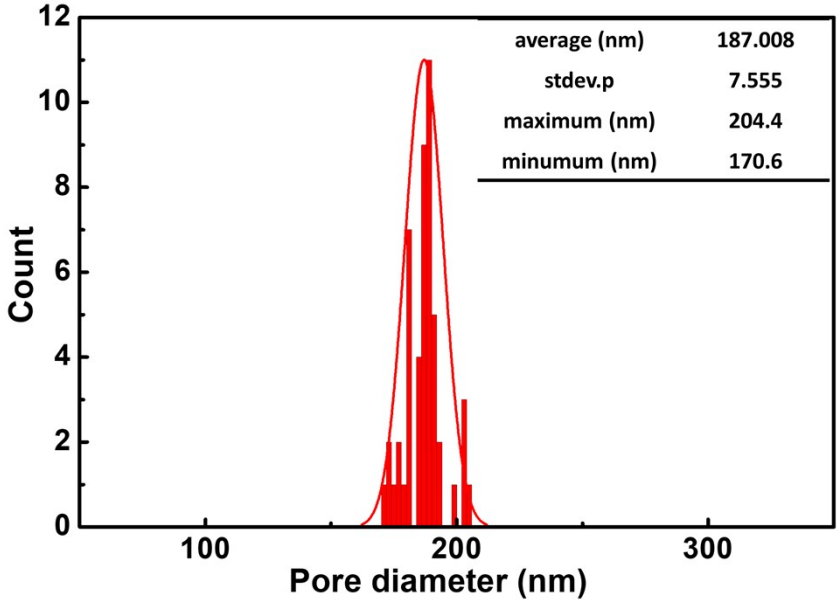

Figure S5. Distribution of the pore diameter in the NUTS. The graph shows a narrow Gaussian curve, and the maximum difference is about 30 nm.

Roughness of the NUTS via AFM

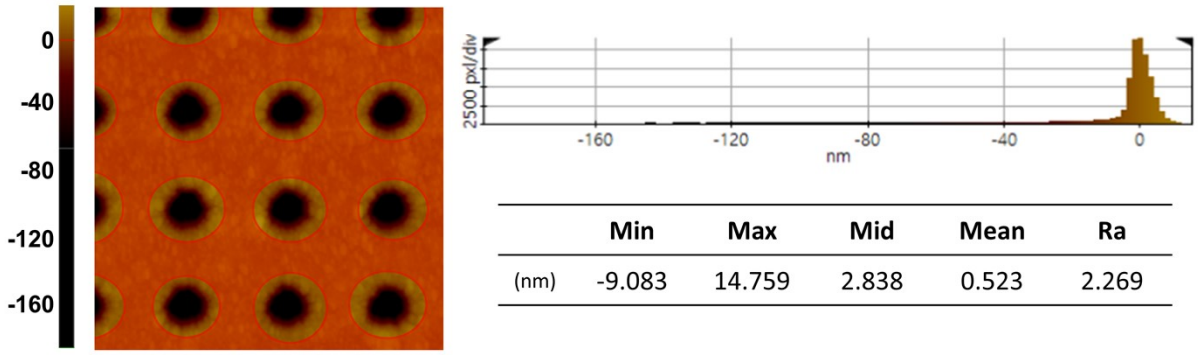

	Min	Max	Mid	Mean	Ra
(nm)	-9.083	14.759	2.838	0.523	2.269

Figure S6. Topography difference of the membrane surface. The average roughness value of the membrane is ~2.27 nm, and the maximum amplitude of roughness (Rpv) is ~23.8 nm. This indicates that the NUTS has a very smooth membrane surface.

Partial fraction of the NUTS by AFM indentation

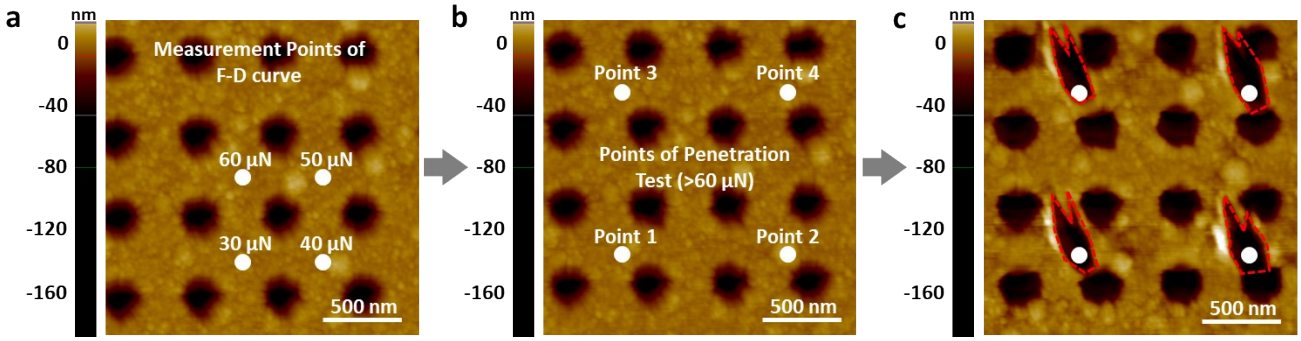

Figure S7. AFM image after the indentation test for various force conditions. The membrane withstood under 60 μN, while the partial fraction occurred over the limited force.

SEM image of membrane after bio-sample filtration

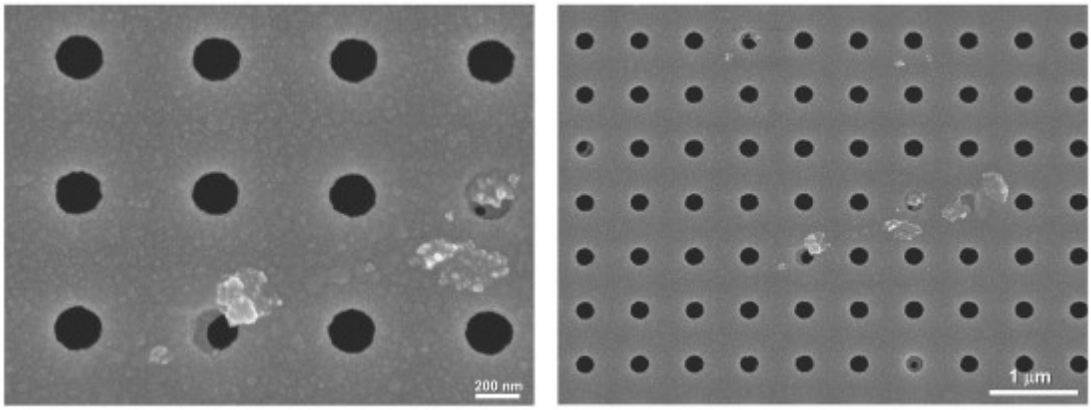

Figure S8. SEM image of the membrane after filtration of the cell-cultured media. The SEM images were measured after filtration of the bio-sample for 5 min. The aggregated molecules were partially adsorbed on the membrane surface. The deposition of particles rarely occurred on the surface, indicating a low chance of cake formation. Although some of the pores had been blocked by the sludge of bio-molecules, most of the pores are open state. Therefore, the permeability of the membrane could be maintained during filtration.

Blocking analysis of bio-sample filtration

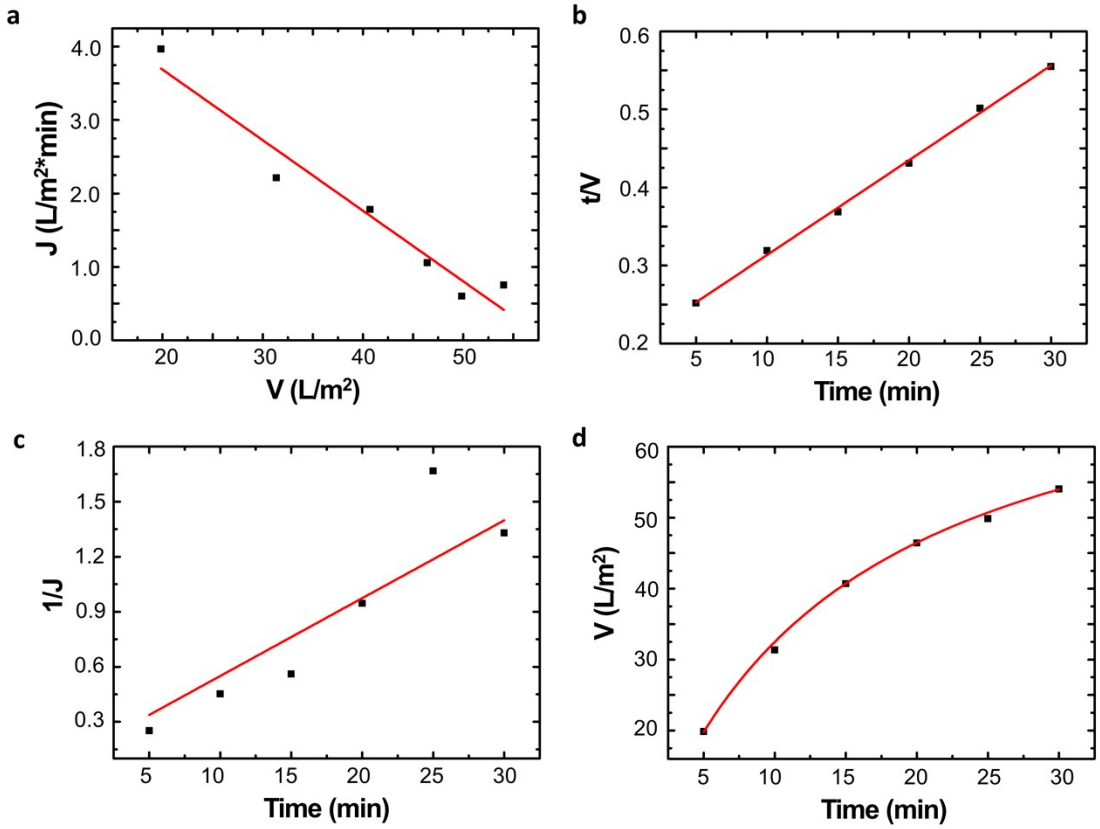

Figure S9. Analysis of the pore blocking mechanism and filtration results using the cell-cultured media (a-c). Linear expressions of modified filtration factors J, V, and t for the calculation of resistance parameters of the pore blocking mechanisms. The values of K_b, K_s, and K_i were 0.0961, 0.0243, and 0.0424, respectively. (d) Drift line of the filtrate volume *via* the linearly combined model of three types pore blocking mechanisms.

Western blot data for the apoptotic body markers

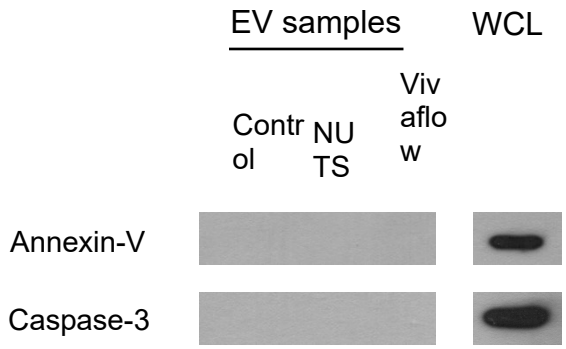

Figure S10. Western blot data of the samples by the markers for apoptotic bodies. Annexin-V and caspase-3 were utilized as markers for apoptotic bodies.[1] They were identified in whole cell lysis (WCL) sample, but there was no detectable signal in whole samples with EVs. The size of the apoptotic body is in the range of 1000–3000 nm, while the EVs used in this study are much smaller size (i.e., under 300 nm). This implies that the preparation of the sample progressed well enough.

Contact angle measurement of the membrane surface

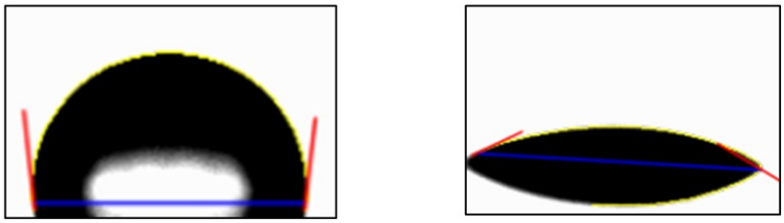

Figure S11. Contact angle measurement of the membrane surface before and after plasma treatment. To determine the hydrophobicity, we measured the contact angles of membrane surfaces before and after oxygen plasma treatment. Before the plasma treatment, the contact angle was 96.74°, and the membrane was a hydrophobic surface. However, after the plasma treatment, the contact angle changed to 27.67°, and the membrane became a hydrophilic surface.

Design of a fluidic channel

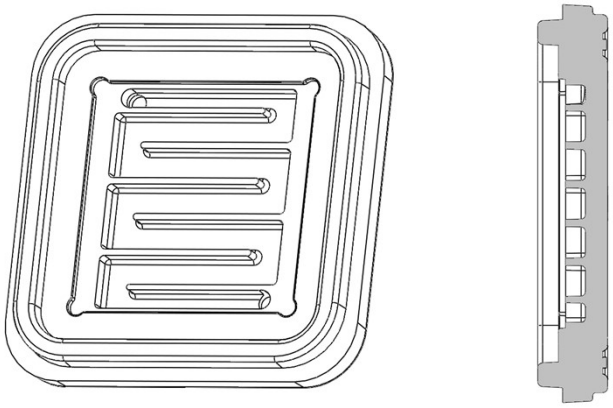

Figure S12. Design of a fluidic channel, which has a meandering shape in a rectangular frame. The channel measures approximately 20 x 24 mm and has seven horizontal lanes of the 3 mm wide channel. The channel has a depth of 2 mm and a symmetrical arrangement. In addition, the first and last lanes are assembled as mock regions without pores on the membrane to prevent abrupt changes in fluidic conditions, thereby regulating a stable fluidic state.

Microarray images of Exoview measurement

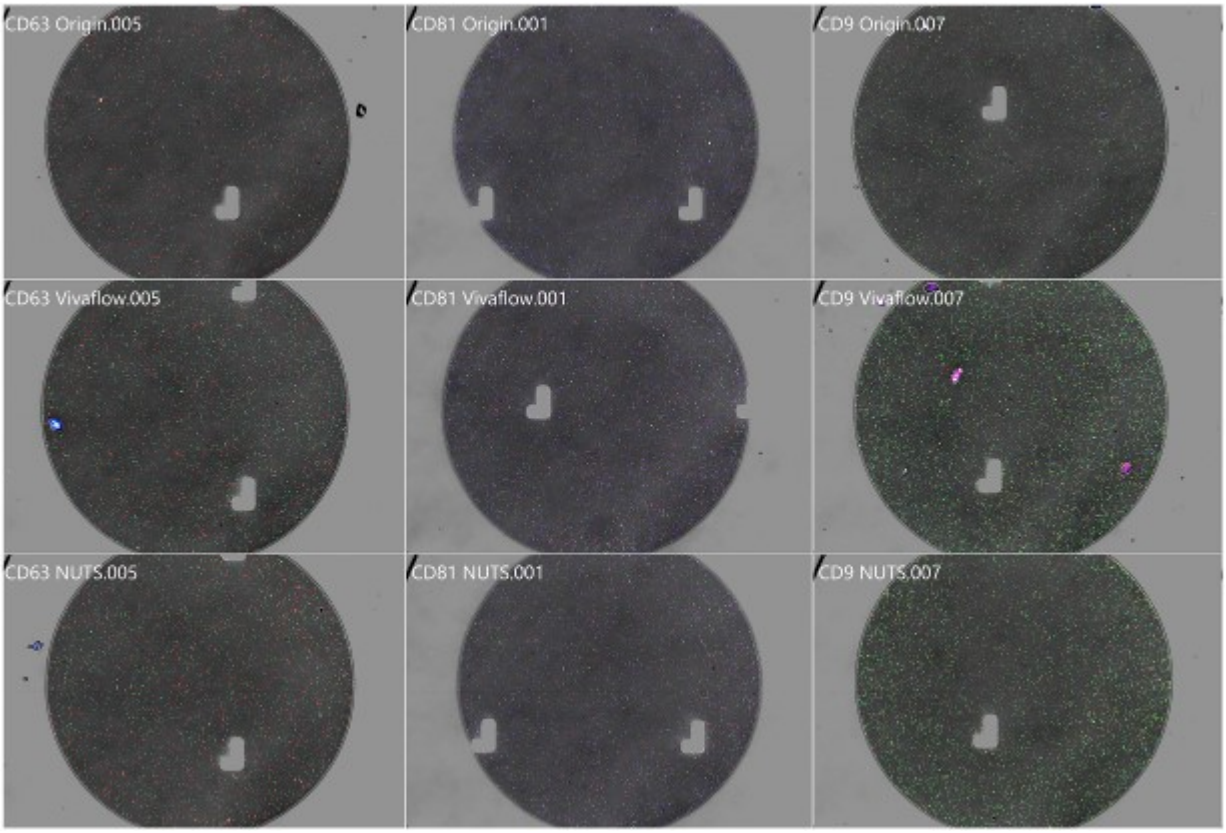

Figure S13. Microarray images of the Exoview measurement. The whole images were merged images of the three types of probe antibodies (i.e., cd63, cd9, and cd81). The intensity conditions are the same as the bar graph in Figure 5.

Reference

1. S. Nomura, T. Taniura and T. Ito, *Int. J. Gen. Med.*, 2020, **13**, 559-568.